

Geophysical Research Letters

RESEARCH LETTER

10.1029/2019GL082951

Key Points:

- Alfvénic turbulence is observed in high-latitude regions associated with Jupiter's auroral emission
- Turbulent magnetic field fluctuations at high latitude map to the central plasma sheet in the inner magnetosphere
- High-latitude fluctuations indicate the presence of significant Alfvénic wave activity at longitudes up to $\sim 90^\circ$ along the Io footprint tail

Supporting Information:

- Supporting Information S1

Correspondence to:

D. J. Gershman,
daniel.j.gershman@nasa.gov

Citation:

Gershman, D. J., Connerney, J. E. P., Kotsiaros, S., DiBraccio, G. A., Martos, Y. M., F.-Viñas, A., et al. (2019). Alfvénic fluctuations associated with Jupiter's auroral emissions. *Geophysical Research Letters*, 46, 7157–7165. <https://doi.org/10.1029/2019GL082951>

Received 21 MAR 2019












Accepted 1 JUN 2019

Accepted article online 5 JUN 2019

Published online 4 JUL 2019

Published 2019. This article is a U.S. Government work and is in the public domain in the USA.

Alfvénic Fluctuations Associated With Jupiter's Auroral Emissions

Daniel J. Gershman¹ , John E. P. Connerney^{2,1} , Stavros Kotsiaros^{1,3} , Gina A. DiBraccio¹ , Yasmina M. Martos^{1,3} , Adolfo F. -Viñas^{1,8,9} , Vincent Hue⁴ , George Clark⁵ , Fran Bagenal⁶ , Steve Levin⁷ , and Scott J. Bolton⁴ 

¹NASA Goddard Space Flight Center, Greenbelt, MD, USA, ²Space Research Corporation, Annapolis, MD, USA,

³Department of Astronomy, University of Maryland, College Park, MD, USA, ⁴Southwest Research Institute, San Antonio, TX, USA, ⁵The Johns Hopkins University Applied Physics Laboratory, Laurel, MD, USA, ⁶Laboratory for Atmospheric and Space Physics, University of Colorado Boulder, Boulder, CO, USA, ⁷Jet Propulsion Laboratory, Pasadena, CA, USA,

⁸Department of Physics, The Catholic University of America, Washington, DC, USA, ⁹Department of Physics, American University, Washington, DC, USA

Abstract The Alfvén wave mode transmits field-aligned currents and large-scale turbulence throughout Jupiter's magnetosphere. Magnetometer data from the Juno spacecraft have provided the first observations of Alfvénic fluctuations along the polar magnetic flux tubes connected to Jupiter's main auroral oval and the Jovian satellites. Transverse magnetic field perturbations associated with Io are observed up to $\sim 90^\circ$ away from main Io footprint, supporting the presence of extended Alfvénic wave activity throughout the Io footprint tail. Additional broadband fluctuations measured equatorward of the statistical auroral oval are composed of incompressible magnetic turbulence that maps to Jupiter's equatorial plasma sheet at radial distances within $\sim 20 R_J$. These fluctuations exhibit a k_{\parallel} power spectrum consistent with strong magnetohydrodynamic turbulence. This turbulence can generate up to $\sim 100 \text{ mW/m}^2$ of Poynting flux to power the Jovian aurora in regions connected to the inner magnetosphere's central plasma sheet.

Plain Language Summary Here we provide the first direct observations of magnetic turbulence near Jupiter's poles. The locations and power of these turbulent fluctuations provide new constraints for modeling the particle acceleration that leads to the generation of Jupiter's aurora. We find that this turbulence provides sufficient energy to produce the aurora at Jupiter, as well as emission associated with Jupiter's moon Io. Constraints on turbulent auroral heating at Jupiter are relevant for analogous processes at other giant magnetospheres such as Saturn, Uranus, and Neptune.

1. Introduction

In magnetohydrodynamics (MHD), Alfvén waves are dispersionless modes whose perturbations are incompressible with respect to the background magnetic field (Alfvén, 1942). These fundamental wave modes travel undamped for large distances, enabling them to set up systems of field-aligned currents at planetary magnetospheres (Hayward & Dungey, 1983; Keiling, 2009; Southwood & Kivelson, 1991). In addition, at Jupiter these waves transmit significant Lorentz forces throughout the magnetosphere that balance the strong centrifugal forcing associated with Jovian rotation (Khurana et al., 2004; Vasyliunas, 1983) and play a significant role in the magnetic connection between the Jovian satellites (Belcher, 1987) and Jupiter's aurora (Clarke et al., 2002, 2004; Connerney & Satoh, 2000). A recent study of Jupiter's high-latitude magnetic field revealed $\sim 300\text{-nT}$ transverse perturbations observed in association with the main auroral oval, providing direct constraints on the structure of such large-scale field-aligned currents (Kotsiaros et al., 2019).

In addition to macroscale magnetic perturbations, significant broadband magnetic turbulence has been reported in the Jovian plasma sheet (Glassmeier, 1995; Ng et al., 2018; Russell et al., 1998; Saur et al., 2002; Tao et al., 2015). These fluctuations were thought to map to Jupiter's high-latitude ionosphere, where their conversion into particle energy has been suggested to serve as a possible generation mechanism of the main Jovian aurora (Saur et al., 2003, 2018). A similar phenomenon known as the “Alfvénic aurora” has been suggested to occur at Earth, where energy transported throughout a turbulent cascade accelerates electrons to sufficient energies to produce auroral emission (Chaston et al., 2008). Such broad, precipitating energetic electron distributions have been reported at Jupiter (Allegrini et al., 2017; Clark et al., 2018;

Connerney, Adriani, et al., 2017; Mauk et al., 2017a, 2017b, 2018), and kinetic simulations of Jovian flux tubes have recently demonstrated that Alfvén waves can provide the needed energization (Damiano et al., 2019). However, without observations of corresponding magnetic fluctuations in the high-latitude magnetosphere, the nature of the turbulent cascade and its relationship to the aurora remain an open issue.

When Voyager 1 flew by Io, the plasma and magnetic field instruments directly observed Alfvénic perturbations (Acuna et al., 1981; Belcher et al., 1981). Gurnett and Goertz (1981) connected these Iogenic Alfvén waves, bouncing back and forth between hemispheres, with Io-triggered radio emissions (Al Warwick, 1979; Carr et al., 1983). These Alfvén waves have been suggested as a mechanism for transmitting power generated by Io's orbital motion around Jupiter to the associated Io footprint (IFP) auroral emission (Gurnett & Goertz, 1981; Hinton et al., 2019; Neubauer, 1980, 1998; Saur, 2004). Some theoretical models (Delamere et al., 2003; Ergun et al., 2009; Hess et al., 2010; Hill & Vasyliunas, 2002; Matsuda et al., 2012; Su et al., 2003) predicted an Alfvénic generation mechanism for the main IFP spot and a steady-state quasi-static electric potential for its tail, while others suggested that Alfvén waves could account for both the main spot and the tail (Bonfond et al., 2009, 2017; Crary & Bagenal, 1997; Jacobsen et al., 2007). Recent thermal particle observations by Juno have reported broad energy distributions of precipitating electrons in these regions (Szalay et al., 2018), indicative of a stochastic acceleration process, though the presence of Alfvénic perturbations in connection to the IFP has not yet been reported.

Here we present observations of broadband Alfvénic fluctuations measured in Jupiter's high-latitude magnetosphere. We use high-resolution magnetometer data collected by the Juno spacecraft over its first dozen perijove (PJ) passes to estimate the spectral power of turbulence in the vicinity of Jupiter's main auroral oval and near the IFP. The spatial variation and spectral index of these fluctuations are then used to constrain their magnetospheric points of origin and to quantify their potential to generate aurora.

2. Data Selection and Analysis

For this study we used fluxgate magnetometer data collected by Juno's magnetic field investigation (MAG; Connerney, Benn, et al., 2017) between July 2016 and April 2018. This time period spanned Juno's first 12 perijove (PJ) passes (i.e., PJ1–PJ12). Data from PJ2 was not available due to the spacecraft's entry into safe mode on approach. The JRM09 model of Jupiter's magnetic field (Connerney et al., 2018) combined with a model magnetodisc (Connerney et al., 1981) was used to map the Juno trajectory to the location of statistical auroral oval and to the footprints of the Jovian moons Io, Europa, and Ganymede (Bonfond et al., 2009, 2012).

Magnetic field vectors were analyzed at the maximum available temporal resolution of 64 vector samples per second. The operational dynamic range of the fluxgate magnetometer varied throughout each PJ in response to the wide dynamic range of ambient magnetic field magnitudes. We restricted our analysis to the highest ranges, namely, ranges “5” and “6,” with nominal dynamic ranges of 4.096 and 16.38 G ($1 \text{ G} = 10^5 \text{ nT}$) which provide resolutions of 12.5 and 50 nT/bit, respectively (Connerney, Benn, et al., 2017). Measured magnetic field vectors for these ranges were expected to be accurate to within one part in 10^4 (Connerney, Adriani, et al., 2017; Connerney, Benn, et al. 2017; Connerney, et al. 2018).

Three-dimensional magnetic field vector measurements were transformed from the rotating sensor coordinate frame into the Jupiter-De-Spun-Sun (JSS) nonrotating frame (i.e., the “JUNO_JSS” frame in Juno SPICE kernels or the Jupiter-Sun-Equatorial frame described by Bagenal et al., 2017). In this coordinate system, the Z axis was oriented along the direction of Jupiter's spin axis, the Y axis was oriented along the direction of the cross product between the spin axis and the unit vector of Jupiter to the Sun, and the X -axis completed the right-handed system.

Power spectral densities (i.e., P_i , where i the quantity of interest) were calculated from discrete fast Fourier transforms of high-resolution Juno magnetic field data. To minimize discontinuities in construction of spectrograms, a Hanning window was applied to the data before transforming into frequency space. Spectrograms of the normalized trace of the power spectral matrix, that is, $P_{Tr} = (P_{Bx} + P_{By} + P_{Bz})/3$, and the spectral power of magnetic field magnitude, that is, $P_{|B|}$, were calculated using successive sets of 30-s samples with 25-s overlap between each interval. These quantities represented the total fluctuation power and compressive fluctuation power, respectively (e.g., Belcher & Davis, 1971; Bavassano et al., 1982).

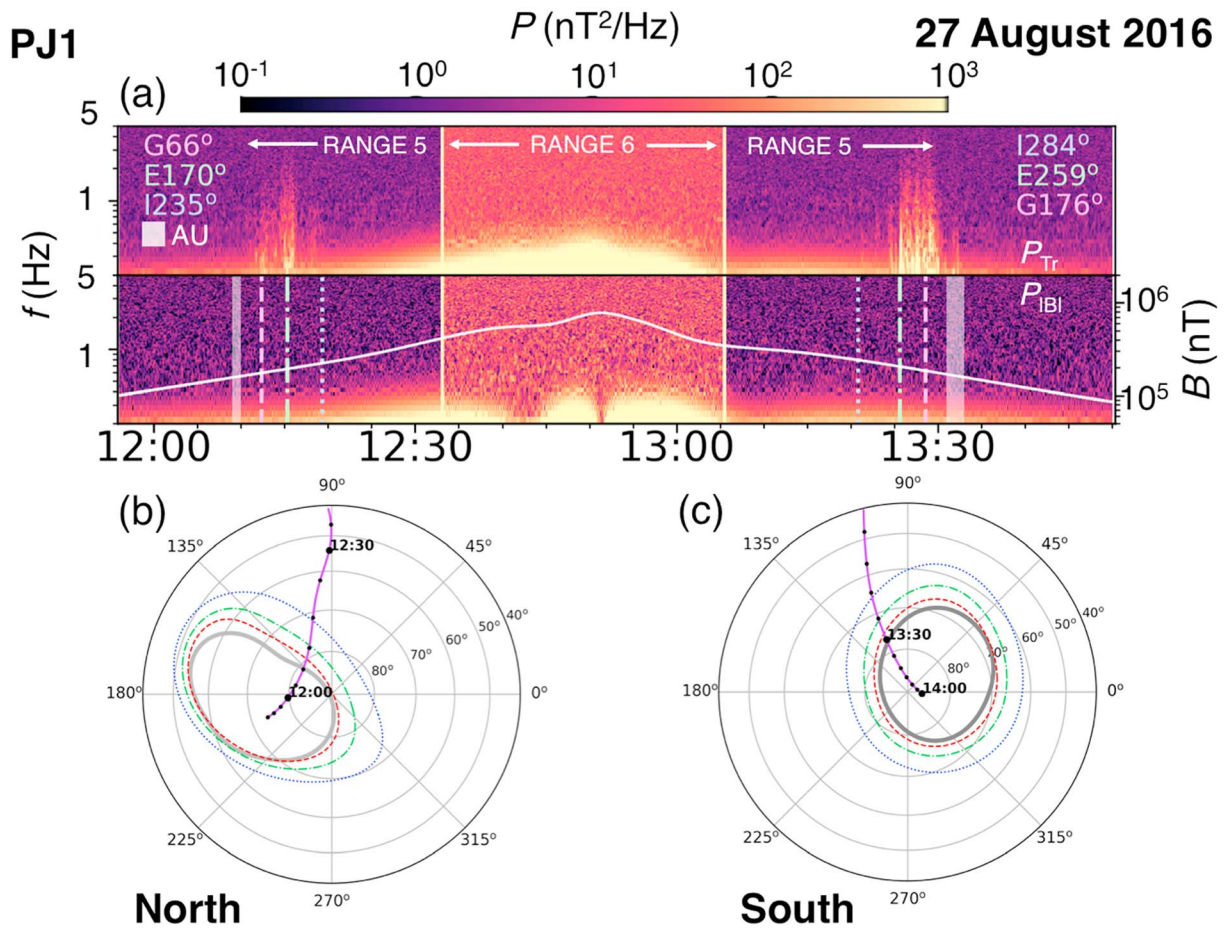


Figure 1. (a) Transverse (top panel) and compressive (bottom panel) magnetic field fluctuation power observed by Juno during PJ1 on 27 August 2016. Vertical colored lines correspond to crossings of the footprint tails of Ganymede (G, red, dashed line), Europa (E, green, dash-dotted line), and Io (I, blue, dotted line). Corresponding longitudinal offsets of the crossing with respect to the main satellite footprint are indicated in the top left and right corners of the transverse spectrogram. The statistical auroral oval (AU) (Bonfond et al., 2012) is indicated with a white shaded region adjacent to the satellite footprint crossing lines. The local magnetic field magnitude is shown as a white solid line in the bottom panel. The spectral noise floor increased between near $\sim 12:30$ and $\sim 13:05$ UT due to the transition of the Juno magnetometer from “range 5” to “range 6” as described in the text. The Juno trajectory is shown over the (b) northern and (c) southern hemispheres as a function of System III latitude and longitude. Mapped locations of the statistical auroral oval and satellite footprints are also shown. Significant transverse fluctuation power was observed just equatorward of the statistical auroral oval. No corresponding power was observed in the magnetic field magnitude, indicating that these fluctuations were Alfvénic in nature.

Frequency in the spacecraft frame (ω_{sc} , rad/s) is related to that in the plasma frame (ω) by the Doppler shift relation, $\omega_{sc} = \omega + \mathbf{k} \cdot \mathbf{V}$, where \mathbf{k} is the wave vector and \mathbf{V} is the relative velocity between the two frames. Here, \mathbf{V} was dominated by the spacecraft velocity, $V_{sc} \sim 50$ km/s (Connerney et al., 2018; Szalay et al., 2018). Often in turbulent analysis, to transform measured frequencies into spatial scales, the Taylor hypothesis is applied, which requires that $|\mathbf{V}| \gg |\omega/k|$, that is, the turbulent eddies can be considered as “frozen” as they advect past the observer (Howes et al., 2014; Matthaeus & Goldstein, 1982; Taylor, 1938). However, in Jupiter’s polar magnetosphere, the field was sufficiently strong to require a semirelativistic description Alfvén wave propagation. In this regime, the Alfvén mode remained nearly dispersionless at fluid scales but propagated with speed $V_A/\sqrt{1+(V_A/c)^2}$, where c is the speed of light and V_A is the typical Alfvén speed of $B/(mn\mu_0)$, with B , m , n , and μ_0 representing to the magnetic field magnitude, particle mass, number density, and vacuum permeability, respectively (Gombosi et al., 2002; Kurbatov et al., 2017; Su et al., 2006). In the high-latitude regions considered here, the Alfvén speed was $\sim c$. Therefore, the Taylor hypothesis was not satisfied, that is, $|\omega/k \sim c| \gg V_{sc}$, even for highly obliquely propagating modes. In this limit,

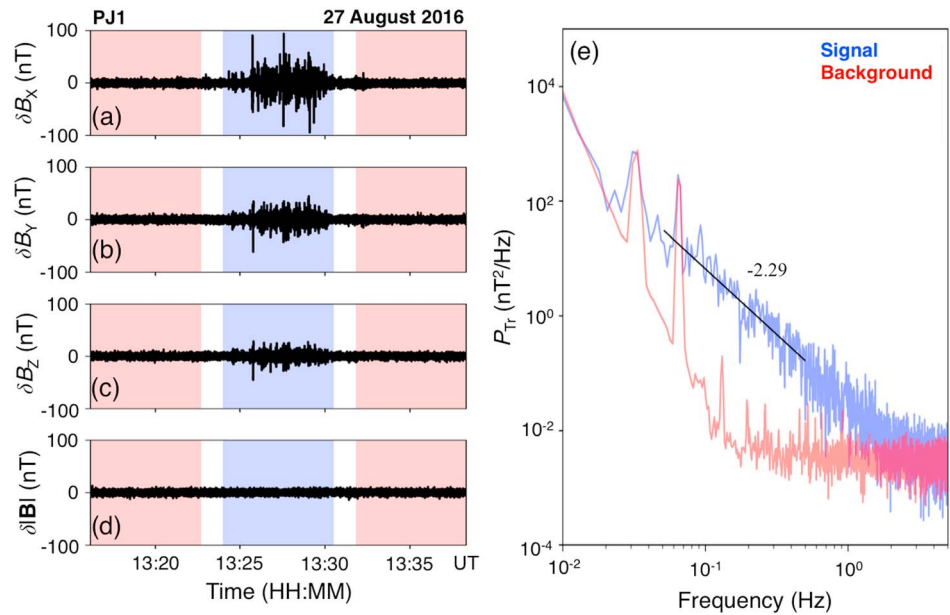


Figure 2. (a–d) Band-pass filtered (0.2–5 Hz) high-resolution magnetometer data from PJ1. Significant perturbations are observed in all components of the magnetic field, with root-mean-square and peak amplitudes of ~ 20 and ~ 100 nT, respectively. No corresponding fluctuations are evident in the magnetic field magnitude, indicating that these variations are Alfvénic in nature. (e) Power spectral density of the measured magnetic field fluctuations (blue shaded region) and background intervals (red shaded region). Peaks in the background at ~ 0.033 and ~ 0.067 Hz corresponded to harmonics of the ~ 30 -s spacecraft spin, and the noise floor corresponded to magnetometer quantization noise. Regions where the signal was significantly above the estimated background were fit with a power law resulting in a spectral index of fluctuations of -2.29 ± 0.09 . Because the frequency in the spacecraft is approximately equal to frequency in the spacecraft frame and the dispersion relation of inertial Alfvén waves is $\omega = c k_{\parallel}$, this spectral index likely corresponded to a turbulent cascade in k_{\parallel} rather than the more often reported k_{\perp} .

frequencies in the spacecraft frame and plasma frame were nearly equal. However, the known dispersion relation of semirelativistic shear Alfvén waves (i.e., $\omega = V_A k \cos(\theta) \sim c k_{\parallel}$, where θ is the angle of propagation with respect to the magnetic field) provided a mechanism to convert frequency to wave vector. The power spectral densities of measured fluctuations in frequency space therefore provided information about the scaling of turbulent energy with k_{\parallel} , rather than the more often measured cascade in k_{\perp} (Glassmeier, 1995; Saur et al., 2003; Tao et al., 2015). Despite having observed frequencies ~ 1 Hz, the wave modes studied here are fluid scale. The kinetic turbulence that directly engages in wave-particle interactions would be measured at significantly higher frequencies.

Finally, the Poynting flux of inertial Alfvén waves was estimated as $\delta B^2 c / \mu_0$ (Saur et al., 2003, 2018), where δB was the root-mean-square (RMS) amplitude of the turbulent fluctuations. Data were band-pass filtered using a fifth-order Butterworth filter with cutoff frequencies 0.2 and 5 Hz, largely isolating fluctuations above the spectral noise floor. The variances of each magnetic field component in a region of interest were then summed to provide an estimate of total fluctuation power. The average fluctuation power in adjacent intervals lacking appreciable Alfvén wave activity was subtracted from this value to provide a background correction. The RMS amplitude δB corresponded to the square root of the resultant sum.

3. Results

An overview of magnetic field fluctuations observed during Juno's PJ1 (27 August 2016) pass is shown in Figure 1. Enhancements of transverse fluctuations were observed in the vicinity of the statistical auroral oval and footprint tails of Io, Europa, and Ganymede in both the northern ($\sim 12:10$ – $12:20$ UT) and southern hemispheres ($\sim 13:26$ – $13:30$ UT). No corresponding compressive fluctuations were observed in either hemisphere. An increased spectral noise floor in the magnetic field data was evident in range 6 due to the increased quantization noise relative to that in range 5.

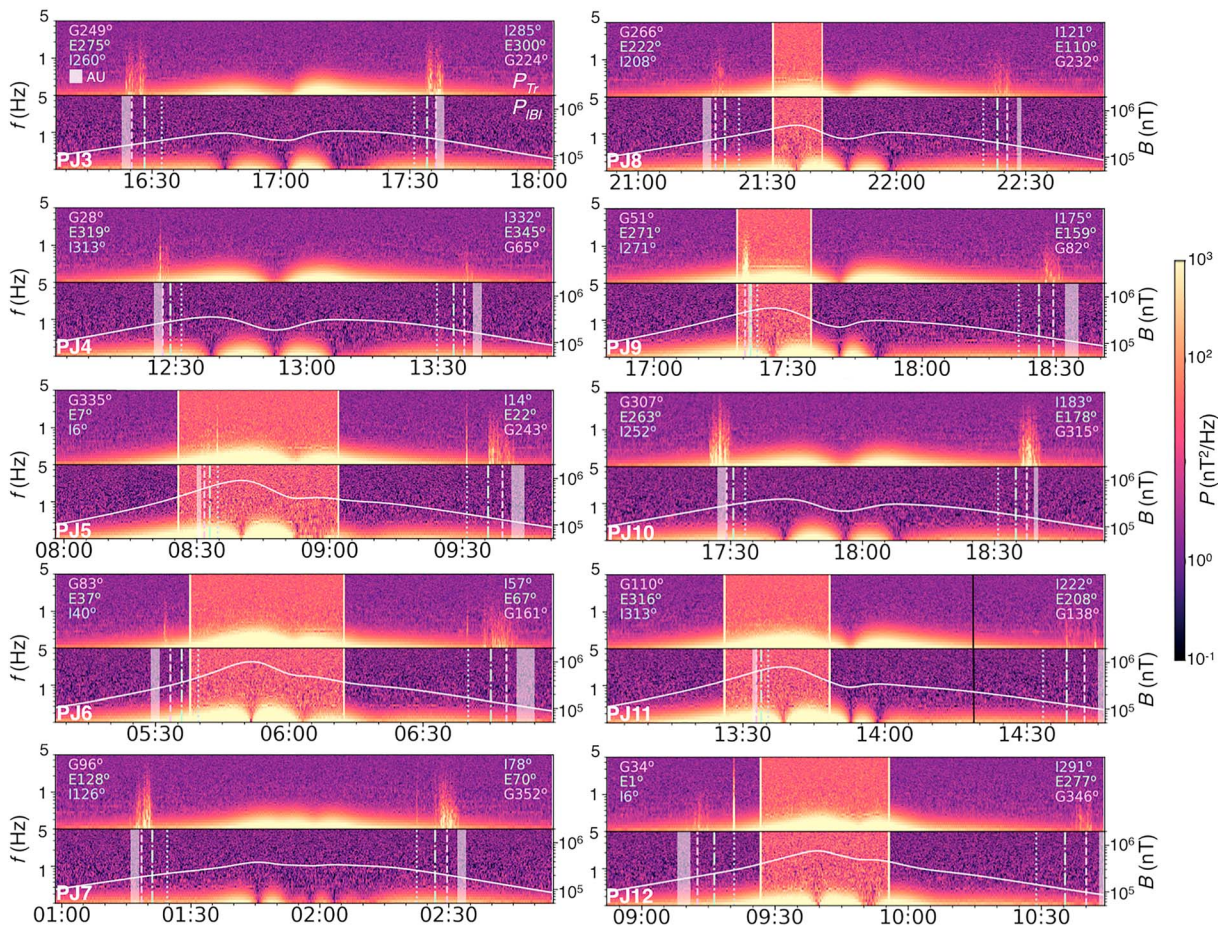


Figure 3. Transverse and compressive magnetic field fluctuation power observed by Juno during PJ3–PJ12. These plots are identical in format to Figure 1, with close-up views and trajectory information for each PJ pass provided in supporting information. As with PJ1, only transverse fluctuation power was observed. This wave power was nearly always localized to regions just equatorward of the statistical auroral oval. Fluctuations specifically associated with crossings of the Io footprint tail were evident in PJ5–PJ7 and PJ12, where the longitudinal distance of Juno from the Io footprint was less than $\sim 90^\circ$. See Figure 1 for legend.

Power spectral densities of the transverse fluctuations observed by Juno from 13:26 to 13:30 UT during PJ1 are shown in Figure 2. Surrounding intervals were used to provide an estimate of the relevant spectral noise. A power law fit to high signal-to-noise data resulted in a spectral index of -2.29 ± 0.09 . Using the relationship $\omega \approx ck_{\parallel}$, the frequency range ~ 0.1 –1 Hz corresponded to parallel wavelengths between ~ 4 – $40 R_J$, where R_J is the equatorial radius of Jupiter, that is, 71,492 km.

Spectrograms from the subsequent ten PJ passes are shown in Figure 3. These data exhibited similar behavior to that observed in PJ1, that is, transverse fluctuations localized near the auroral zones, with no observable compressive component. Close-up images for each PJ in the same format as Figure 1 were included as supporting information. In total, these 11 PJ passes spanned a full range of System III longitudes, with transverse fluctuation power observed on nearly every crossing of the auroral field lines, with the exception of PJ11 near $\sim 13:30$ UT.

Finally, significant fluctuation power was evident in Figure 3 associated with the IFP tail. The Poynting flux was estimated for six intervals when Juno crossed within 90° in longitude from the IFP. These fluxes, as well as the observed altitude and longitudinal distance from the IFP, are shown for each interval in Figure 4. The strongest wave power of $\sim 1,000$ mW/m² was measured during PJ12, when Juno passed within $\sim 6^\circ$ of the IFP. Weaker Poynting fluxes of ~ 10 mW/m² were observed up to $\sim 90^\circ$ in the IFP tail during PJ 6. The altitudes of IFP tail crossings varied significantly from ~ 0.2 to $\sim 2 R_J$. PJ5 and PJ6 crossed the IFP tail at nearly the same altitude of $\sim 0.7 R_J$ but at longitudinal distances of 14° and 78° , respectively, resulting in a difference in fluctuation power by an order of magnitude.

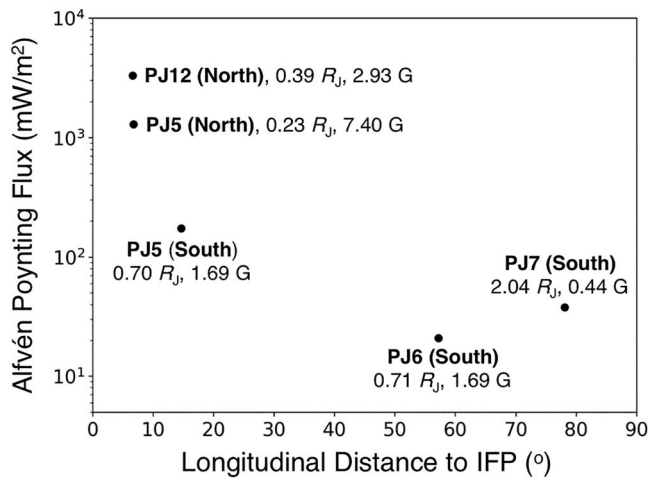


Figure 4. Io-associated Alfvén Poynting flux calculated from high-resolution magnetometer data as a function of longitudinal distance of Juno from the IFP. As described in the text, Poynting flux was estimated using $\delta B^2 c / \mu_0$, where δB is the root-mean-square amplitude of magnetic field fluctuations with frequencies between 0.2 and 5 Hz (frequency range shown in Figure 3). The spacecraft altitude and average magnetic field magnitude at the time of each observation are indicated with each data point. The strongest wave activity was observed closest to the IFP, with weaker, but measurable, fluctuations observed up to $\sim 90^\circ$ away. Fluctuation power was below the spectral noise floor for crossings where the longitudinal distance exceeded 90° (see Figure 3 and supporting information).

4. Discussion

The presented polar magnetic field data provide measurable evidence of significant Alfvénic wave activity (i.e., $\sim 10 mW/m^2$) at IFP tail longitudes up to $\sim 90^\circ$, with up to $\sim 1,000 mW/m^2$ a few degrees from the main Io spot. This range of Poynting fluxes is consistent with precipitating electron fluxes determined by Szalay et al. (2018) for PJ5–PJ7 and typical UV auroral brightness values (Bonfond et al., 2009, 2012), suggesting that Alfvén wave activity is sufficient to generate the IFP tail. This wave power was observed at higher frequencies in the Juno magnetometer data (i.e., between ~ 0.2 and 5 Hz) and was therefore not apparent in Juno spin-averaged data (e.g., Szalay et al., 2018).

Broadband Alfvénic turbulence was observed at all System III longitudes but was confined to within polar latitudes immediately equatorward of the statistical auroral oval. The broadband fluctuations observed in PJ1 aligned with the broad-energy electron signatures reported by the energetic particle instruments (Allegrini et al., 2017; Clark et al., 2018; Mauk et al., 2017a, 2017b, 2018). No corresponding fluctuations were observed in concert with the discrete-energy electron signatures described by Mauk et al. (2017a, 2017b, 2018). The RMS value of the band-pass filtered Alfvén turbulence in Figure 1 was ~ 20 nT, corresponding to an average Poynting flux of $\sim 80 mW/m^2$. This value is in good agreement with fluxes of energetic electrons reported by Mauk et al., 2017b, suggesting that Alfvénic turbulence provides a sufficient source of acceleration of electrons generating auroral emission at Jupiter as discussed by Saur et al. (2003, 2018) and Damiano et al. (2019).

The spatial localization of broadband fluctuations observed in the high-latitude regions suggested that they were related to a narrowly focused latitudinal band of auroral emission. The observed polar turbulence mapped to Jupiter’s central plasma sheet between the Io torus and the stretched magnetodisc current sheet, that is, equatorial distances between ~ 10 and $20 R_J$, as evidenced by magnetic field modeling and examination of thermal plasma data during this time period (e.g., Figure 1 in Szalay et al., 2017). Appreciable power dissipation within polar latitudes between the IFT footprint and the main aurora has also been established by remote observations of H_3^+ emissions (Satoh et al., 1996; Satoh & Connerney, 1999). Plasma sheet turbulence produced beyond $\sim 20 R_J$ appeared to remain confined to lower latitudes, with no corresponding observations discernable in the polar data. The turbulent energy at these larger distances therefore should have resulted in the heating of magnetospheric plasma rather than the acceleration of auroral electrons (Saur et al., 2018).

At the equator, wave phase speeds are small compared to plasma convection speeds such that measured magnetic field fluctuations map to a spectrum in k_\perp . At high-latitudes, where the phase speeds are on the order of the speed of light, measured magnetic field fluctuations map to a spectrum in k_\parallel . The measured inertial range $\sim k_\parallel^{-2.29 \pm 0.09}$ spectrum over the poles suggested that the turbulence along the field line could be consistent with a critically balanced (i.e., strong MHD turbulence) Kolmogorov cascade (i.e., $E \sim k_\perp^{-5/3}$) (Goldreich & Sridhar, 1995). “Critical balance” assumes that the linear wave time scale and nonlinear energy transfer time scale are comparable in the region where the energy transfer takes place. At Jupiter, this interaction was likely confined to low latitudes (Saur et al., 2003). In critically balanced Kolmogorov turbulence, the perpendicular and parallel inertial range cascades exhibit spectral indices of $-5/3$ and -2 , respectively. Such cascades are often observed in the solar wind (Chen et al., 2011; Wicks et al., 2011). Kolmogorov-like k_\perp spectra have been reported in Jupiter’s equatorial plasma sheet in the vicinity of $\sim 20 R_J$ (Glassmeier, 1995; Tao et al., 2015; Ng et al., 2018). Because the turbulent fluctuations are contained within a given flux tube, an inertial range $k_\perp^{-5/3}$ measured at the equator would be equivalent to an inertial range k_\parallel^{-2} spectrum measured at high latitudes. The observed parallel spectrum was somewhat steeper than k_\parallel^{-2} (i.e., closer to $k_\parallel^{-7/3}$) indicating that the cascade may not have been fully developed. Even if the critical balance assumption is not fully valid, the definitive measurement of an inertial range k_\parallel spectrum here suggested that weak

MHD turbulence theory may not have provided a complete description of the turbulence in this region, as it excludes the presence of such a parallel cascade (Galtier et al., 2000). However, this constraint likely only places modest limitations on the dissipation rates estimated by Saur et al. (2003, 2018), who assumed weak turbulence framework for turbulence at Jupiter.

5. Conclusions

We have reported observations of broadband Alfvénic waves in Jupiter's polar magnetosphere that demonstrated the following: (1) the power spectrum of high-latitude fluctuations can exhibit a $k_{\parallel}^{-2.29 \pm 0.09}$ dependence, suggesting that the observations were consistent with strong MHD turbulence; (2) Alfvénic turbulence maps to regions of Jupiter's inner magnetosphere where the magnetic fields remained relatively dipolar and provides up to ~ 100 mW/m² of power available for stochastic particle acceleration and subsequent auroral generation; (3) Alfvénic activity along the IFP tail provides up to $\sim 1,000$ mW/m² close to the Io flux tube, with ~ 10 mW/m² observable up to $\sim 90^\circ$ away from the tail; (4) Alfvén waves likely play a significant role in the generation of both the main aurora at Jupiter as well as extended IFP tail.

Acknowledgments

Juno data are publicly available from NASA's Planetary Data System as part of the JNO-J-3-FGM-CAL-V1.0.0 data set for the Juno MAG instrument. This work was supported by the Juno mission.

References

- Acuna, M. H., Neubauer, F. M., & Ness, N. F. (1981). Standing Alfvén wave current system at Io: Voyager observations. *Journal of Geophysical Research*, *86*(A10), 8513–8521. <https://doi.org/10.1029/JA086iA10p08513>
- Alfvén, H. (1942). Existence of electromagnetic-hydrodynamic waves. *Nature*, *150*(3805), 405–406. <https://doi.org/10.1038/150405d0>
- Allegrini, F., Bagenal, F., Bolton, S., Connerney, J., Clark, G., Ebert, R. W., et al. (2017). Electron beams and loss cones in the auroral regions of Jupiter. *Geophysical Research Letters*, *44*, 7131–7139. <https://doi.org/10.1002/2017GL073180>
- Bagenal, F., Adriani, A., Allegrini, F., Bolton, S. J., Bonfond, B., Bunce, E. J., et al. (2017). Magnetospheric science objectives of the Juno mission. *Space Science Reviews*, *213*(1-4), 219–287. <https://doi.org/10.1007/s11214-014-0036-8>
- Bavassano, B., Dobrowolny, M., Mariani, F., & Ness, N. F. (1982). Radial evolution of power spectra of interplanetary Alfvénic turbulence. *Journal of Geophysical Research*, *87*(A5), 3617–3622. <https://doi.org/10.1029/JA087iA05p03617>
- Belcher, J. W. (1987). The Jupiter-Io connection: An Alfvén engine in space. *Science*, *238*(4824), 170–176. <https://doi.org/10.1126/science.238.4824.170>
- Belcher, J. W., & Davis, L. (1971). Large-amplitude Alfvén waves in the interplanetary medium, 2. *Journal of Geophysical Research*, *76*(16), 3534–3563. <https://doi.org/10.1029/JA076i016p03534>
- Belcher, J. W., Goertz, C. K., Sullivan, J. D., & Acuna, M. H. (1981). Plasma observations of the Alfvén wave generated by Io. *Journal of Geophysical Research*, *86*(A10), 8508–8512. <https://doi.org/10.1029/JA086iA10p08508>
- Bonfond, B., Grodent, D., Gérard, J.-C., Radioti, A., Dols, V., Delamere, P. A., & Clarke, J. T. (2009). The Io UV footprint: Location, inter-spot distances and tail vertical extent. *Journal of Geophysical Research*, *114*(A7), A07224. <https://doi.org/10.1029/2009JA014312>
- Bonfond, B., Grodent, D., Gérard, J.-C., Stallard, T., Clarke, J. T., Yoneda, M., et al. (2012). Auroral evidence of Io's control over the magnetosphere of Jupiter. *Geophysical Research Letters*, *39*, L01105. <https://doi.org/10.1029/2011GL050253>
- Bonfond, B., Saur, J., Grodent, D., Badman, S. V., Bisikalo, D., Shematovich, V., et al. (2017). The tails of the satellite auroral footprints at Jupiter. *Journal of Geophysical Research: Space Physics*, *122*, 7985–7996. <https://doi.org/10.1002/2017JA024370>
- Carr, T. D., Desch, M. D., & Alexander, J. K. (1983). Phenomenology of magnetospheric radio emissions. In A. J. Dessler (Ed.), *Physics of the Jovian Magnetosphere*, (pp. 226–284). Cambridge: Cambridge University Press. <https://doi.org/10.1017/CBO9780511564574.009>
- Chaston, C. C., Salem, C., Bonnell, J. W., Carlson, C. W., Ergun, R. E., Strangeway, R. J., & McFadden, J. P. (2008). The turbulent Alfvénic aurora. *Physical Review Letters*, *100*(17). <https://doi.org/10.1103/PhysRevLett.100.175003>
- Chen, C. H. K., Mallet, A., Yousef, T. A., Schekochihin, A. A., & Horbury, T. S. (2011). Anisotropy of Alfvénic turbulence in the solar wind and numerical simulations. *Monthly Notices of the Royal Astronomical Society*, *415*(4), 3219–3226. <https://doi.org/10.1111/j.1365-2966.2011.18933.x>
- Clark, G., Tao, C., Mauk, B. H., Nichols, J., Saur, J., Bunce, E. J., et al. (2018). Precipitating electron energy flux and characteristic energies in Jupiter's main auroral region as measured by Juno/JEDI. *Journal of Geophysical Research: Space Physics*, *123*, 7554–7567. <https://doi.org/10.1029/2018JA025639>
- Clarke, J. T., Ajello, J., Ballester, G., Ben Jaffel, L., Connerney, J., Gérard, J. C., et al. (2002). Ultraviolet auroral emissions from the magnetic footprints of Io, Ganymede, and Europa on Jupiter. *Nature*, *415*(6875), 997–1000. <https://doi.org/10.1038/415997a>
- Clarke, J. T., Grodent, D., Cowley, S., Bunce, E., Connerney, J., & Satoh, T. (2004). *Jupiter's aurora, in Jupiter: The planet, satellites, and magnetosphere*, (pp. 639–670). Cambridge, U. K: Cambridge Univ. Press.
- Connerney, J. E. P., Acuna, M. H., & Ness, N. F. (1981). Modeling the Jovian current sheet and inner magnetosphere. *Journal of Geophysical Research*, *86*(A10), 8370–8384. <https://doi.org/10.1029/JA086iA10p08370>
- Connerney, J. E. P., Adriani, A., Allegrini, F., Bagenal, F., Bolton, S. J., Bonfond, B., et al. (2017). Jupiter's magnetosphere and aurorae observed by the Juno spacecraft during its first polar orbits. *Science*, *356*(6340), 826–832. <https://doi.org/10.1126/science.aam5928>
- Connerney, J. E. P., Benn, M., Bjarno, J. B., Denver, T., Espley, J., Jorgensen, J. L., et al. (2017). The Juno magnetic field investigation. *Space Science Reviews*, *213*(1-4), 39–138. <https://doi.org/10.1007/s11214-017-0334-z>
- Connerney, J. E. P., Kotsiaros, S., Oliverson, R. J., Espley, J. R., Joergensen, P. S., et al. (2018). A new model of Jupiter's magnetic field from Juno's first nine orbits. *Geophysical Research Letters*, *45*, 2590–2596. <https://doi.org/10.1002/2018GL077312>
- Connerney, J. E. P., & Satoh, T. (2000). The H3+ ion: A remote diagnostic of the Jovian magnetosphere. *Philosophical Transactions of the Royal Society A*, *358*(1774), 2471–2483. <https://doi.org/10.1098/rsta.2000.0661>
- Crary, F. J., & Bagenal, F. (1997). Coupling the plasma interaction at Io to Jupiter. *Geophysical Research Letters*, *24*(17), 2135–2138. <https://doi.org/10.1029/97GL02248>
- Damiano, P. A., Delamere, P. A., Stauffer, B., Ng, C.-S., & Johnson, J. R. (2019). Kinetic Simulations of Electron Acceleration by Dispersive Scale Alfvén Waves in Jupiter's Magnetosphere. *Geophysical Research Letters*, *46*(6), 3043–3051. <https://doi.org/10.1029/2018gl081219>

- Delamere, P. A., Bagenal, F., Ergun, R. E., & Su, Y. J. (2003). Momentum transfer between the Io plasma wake and Jupiter's ionosphere. *Journal of Geophysical Research*, *108*(A6), 1241. <https://doi.org/10.1029/2002JA009530>
- Ergun, R. E., Ray, L., Delamere, P. A., Bagenal, F., Dols, V., & Su, Y. J. (2009). Generation of parallel electric fields in the Jupiter-Io torus wake region. *Journal of Geophysical Research*, *114*, A05201. <https://doi.org/10.1029/2008JA013968>
- Galtier, S., Nazarenko, S. V., Newell, A. C., & Pouquet, A. (2000). A weak turbulence theory for incompressible magnetohydrodynamics. *Journal of Plasma Physics*, *63*(5), 447–488. <https://doi.org/10.1017/S0022377899008284>
- Glassmeier, K. H. (1995). Ultralow-frequency pulsations: Earth and Jupiter compared. *Advances in Space Research*, *164*, 209.
- Goldreich, P., & Sridhar, S. (1995). Toward a theory of interstellar turbulence. II. Strong Alfvénic turbulence. *The Astrophysical Journal*, *438*, 763–775. <https://doi.org/10.1086/175121>
- Gombosi, T. I., Tóth, G., De Zeeuw, D. L., Hansen, K. C., Kabin, K., & Powell, K. G. (2002). Semi-relativistic magnetohydrodynamics and physics-based convergence acceleration. *Journal of Computational Physics*, *177*(1), 176–205. <https://doi.org/10.1006/jcph.2002.7009>
- Gurnett, D. A., & Goertz, C. K. (1981). Multiple Alfvén wave reflections excited by Io origin of the Jovian decametric arcs. *Journal of Geophysical Research*, *86*(A2), 717–722. <https://doi.org/10.1029/JA086iA02p00717>
- Hayward, D., & Dungey, J. W. (1983). An Alfvén wave approach to auroral field-aligned currents. *Planetary and Space Science*, *31*(5), 579–585. [https://doi.org/10.1016/0032-0633\(83\)90047-8](https://doi.org/10.1016/0032-0633(83)90047-8)
- Hess, S. L. G., Delamere, P., Dols, V., Bonfond, B., & Swift, D. (2010). Power transmission and particle acceleration along the Io flux tube. *Journal of Geophysical Research Space Physics*, *115*, A06205. <https://doi.org/10.1029/2009ja014928>
- Hill, T. W., & Vasyliunas, V. M. (2002). Jovian auroral signature of Io's corotational wake. *Journal of Geophysical Research*, *107*(A12), 1464. <https://doi.org/10.1029/2002JA009514>
- Hinton, P. C., Bagenal, F., & Bonfond, B. (2019). Alfvén wave propagation in the Io plasma torus. *Geophysical Research Letters*, *46*, 1242–1249. <https://doi.org/10.1029/2018GL081472>
- Howes, G. G., Klein, K. G., & TenBarge, J. M. (2014). Validity of the Taylor hypothesis for linear kinetic waves in the weakly collisional solar wind. *The Astrophysical Journal*, *789*(2), 106. <https://doi.org/10.1088/0004-637X/789/2/106>
- Jacobsen, S., Neubauer, F. M., Saur, J., & Schilling, N. (2007). Io's nonlinear MHD-wave field in the heterogeneous Jovian magnetosphere. *Geophysical Research Letters*, *34*, L10202. <https://doi.org/10.1029/2006GL029187>
- Keiling, A. (2009). Alfvén waves and their roles in the dynamics of the Earth's magnetotail: A review. *Space Science Reviews*, *142*(1–4), 73–156. <https://doi.org/10.1007/s11214-008-9463-8>
- Khurana, K. K., Kivelson, M. G., Vasyliunas, V. M., Krupp, N., Woch, J., Lagg, A., et al. (2004). The configuration of Jupiter's magnetosphere. In F. Bagenal, T. E. Dowling, & W. B. McKinnon (Eds.), *Jupiter: The planet, satellites and magnetosphere* (p. 593, chap. 24). New York: Cambridge Univ. Press.
- Kotsiaros, S., Connerney, J. E. P., Clark, G., Allegrini, F., Gladstone, G. R., Kurth, W. S., et al. (2019). Birkeland currents in Jupiter's magnetosphere observed by the polar-orbiting Juno spacecraft. *Nature Astronomy*. <https://doi.org/10.1038/s41550-019-0819-7>
- Kurbatov, E. P., Zhilkin, A. G., & Bisikalo, D. V. (2017). Modified magnetohydrodynamics model with wave turbulence: Astrophysical applications. *Physics-Uspekhi*, *60*, 8, 798. <https://doi.org/10.3367/UFNe.2017.01.038063>
- Matsuda, K., Terada, N., Katoh, Y., & Misawa, H. (2012). A simulation study of the current-voltage relationship of the Io tail aurora. *Journal of Geophysical Research*, *117*, A10214. <https://doi.org/10.1029/2012JA017790>
- Matthaeus, W. H., & Goldstein, M. L. (1982). Measurement of the rugged invariants of magnetohydrodynamic turbulence in the solar wind. *Journal of Geophysical Research*, *87*(A8), 6011–6028. <https://doi.org/10.1029/JA087iA08p06011>
- Mauk, B. H., Haggerty, D. K., Paranicas, C., Clark, G., Kollmann, P., Rymer, A. M., et al. (2017a). Discrete and broadband electron acceleration in Jupiter's powerful aurora. *Nature*, *549*(7670), 66–69. <https://doi.org/10.1038/nature23648>
- Mauk, B. H., Haggerty, D. K., Paranicas, C., Clark, G., Kollmann, P., Rymer, A. M., et al. (2017b). Juno observations of energetic charged particles over Jupiter's polar regions: Analysis of mono- and bi-directional electron beams. *Geophysical Research Letters*, *44*, 4410–4418. <https://doi.org/10.1002/2016GL072286>
- Mauk, B. H., Haggerty, D. K., Paranicas, C., Clark, G., Kollmann, P., Rymer, A. M., et al. (2018). Diverse electron and ion acceleration characteristics observed over Jupiter's main aurora. *Geophysical Research Letters*, *45*(3), 1277–1285. <https://doi.org/10.1002/2017GL076901>
- Neubauer, F. M. (1980). Nonlinear standing Alfvén wave current system at Io—Theory. *Journal of Geophysical Research*, *85*(A3), 1171–1178. <https://doi.org/10.1029/JA085iA03p01171>
- Neubauer, F. M. (1998). The sub-Alfvénic interaction of the Galilean satellites with the Jovian magnetosphere. *Journal of Geophysical Research*, *103*, 19,843–19,866. <https://doi.org/10.1029/97JE03370>
- Ng, C. S., Delamere, P. A., Kaminker, V., & Damiano, P. A. (2018). Radial Transport and Plasma Heating in Jupiter's Magnetodisc. *Journal of Geophysical Research: Space Physics*, *123*(8), 6611–6620. <https://doi.org/10.1029/2018ja025345>
- Russell, C. T., Huddleston, D. E., Khurana, K. K., & Kivelson, M. G. (1998). The fluctuating magnetic field in the middle Jovian magnetosphere: Initial Galileo observations. *Planetary and Space Science*, *47*(1–2), 133–142. [https://doi.org/10.1016/S0032-0633\(98\)00092-0](https://doi.org/10.1016/S0032-0633(98)00092-0)
- Satoh, T., & Connerney, J. E. P. (1999). Jupiter's H₃⁺ emissions viewed in corrected Jovimagnetic coordinates. *Icarus*, *141*(2), 236–252. <https://doi.org/10.1006/icar.1999.6173>
- Satoh, T., Connerney, J. E. P., & Baron, R. (1996). Emission source model of Jupiter's H₃⁺ aurorae: A Generalized inverse analysis of images. *Icarus*, *122*(1), 1–23. <https://doi.org/10.1006/icar.1996.0106>
- Saur, J. (2004). Turbulent heating of Jupiter's magnetosphere. *The Astrophysical Journal Letters*, *602*(2), L137–L140. <https://doi.org/10.1086/382588>
- Saur, J., Janser, S., Schreiner, A., Clark, G., Mauk, B. H., Kollmann, P., et al. (2018). Wave-particle interaction of Alfvén waves in Jupiter's magnetosphere: Auroral and magnetospheric particle acceleration. *Journal of Geophysical Research: Space Physics*, *123*, 9560–9573. <https://doi.org/10.1029/2018JA025948>
- Saur, J., Politano, H., Pouquet, A., & Matthaeus, W. H. (2002). Evidence for weak MHD turbulence in the middle magnetosphere of Jupiter. *Astronomy and Astrophysics*, *386*(2), 699–708. <https://doi.org/10.1051/0004-6361:20020305>
- Saur, J., Pouquet, A., & Matthaeus, W. H. (2003). An acceleration mechanism for the generation of the main auroral oval on Jupiter. *Geophysical Research Letters*, *30*(5), 1260. <https://doi.org/10.1029/2002GL015761>
- Southwood, D. J., & Kivelson, M. G. (1991). An approximate description of field-aligned currents in a planetary magnetic field. *Journal of Geophysical Research*, *96*(A1), 67–75. <https://doi.org/10.1029/90JA01806>
- Su, Y.-J., Ergun, R. E., Bagenal, F., & Delamere, P. A. (2003). Io-related Jovian auroral arcs: Modeling parallel electric fields. *Journal of Geophysical Research*, *108*(A2), 1094. <https://doi.org/10.1029/2002JA009247>

- Su, Y.-J., Jones, S. T., Ergun, R. E., Bagenal, F., Parker, S. E., Delamere, P. A., & Lysak, R. L. (2006). Io-Jupiter interaction: Alfvén wave propagation and ionospheric Alfvén resonator. *Journal of Geophysical Research*, *111*, A06211. <https://doi.org/10.1029/2005JA011252>
- Szalay, J. R., Allegrini, F., Bagenal, F., Bolton, S., Clark, G., Connerney, J. E. P., et al. (2017). Plasma measurements in the Jovian polar region with Juno/JADE. *Geophysical Research Letters*, *44*, 7122–7130. <https://doi.org/10.1002/2017GL072837>
- Szalay, J. R., Bonfond, B., Allegrini, F., Bagenal, F., Bolton, S., Clark, G., et al. (2018). In situ observations connected to the Io footprint tail aurora. *Journal of Geophysical Research: Planets*, *123*, 3061–3077. <https://doi.org/10.1029/2018JE005752>
- Tao, C., Sahraoui, F., Fontaine, D., Patoul, J., Chust, T., Kasahara, S., & Retinò, A. (2015). Properties of Jupiter's magnetospheric turbulence observed by the Galileo spacecraft. *Journal of Geophysical Research: Space Physics*, *120*, 2477–2493. <https://doi.org/10.1002/2014JA020749>
- Taylor, G. I. (1938). The Spectrum of Turbulence. *Proceedings of the Royal Society of London. Series A*, *164*(919), 476–490. <https://doi.org/10.1098/rspa.1938.0032>
- Vasyliunas, V. M. (1983). In A. J. Dessler (Ed.), *Plasma distribution and flow, Physics of the Jovian Magnetosphere*, (pp. 395–453). New York: Cambridge Univ. Press.
- Warwick, J. W., Pearce, J. B., Riddle, A. C., Alexander, J. K., Desch, M. D., Kaiser, M. L., et al. (1979). Voyager 1 planetary radio astronomy observations near Jupiter. *Science*, *204*(4396), 995–998. <https://doi.org/10.1126/science.204.4396.995>
- Wicks, R. T., Horbury, T. S., Chen, C. H. K., & Schekochihin, A. A. (2011). Anisotropy of imbalanced Alfvénic turbulence in fast solar wind. *Physical Review Letters*, *106*(4), 045001. <https://doi.org/10.1103/PhysRevLett.106.045001>